Oak decaying wood harbors taxonomically and functionally different bacterial communities in sapwood and heartwood

S. Mieszkin, P. Richet, C. Bach, C. Lambrot, Laurent Augusto, Marc Buée, S. Uroz

Title

Oak decaying wood harbors taxonomically and functionally different bacterial communities in sapwood and heartwood

Authors

S. Mieszkin[a,*], P. Richet [a], C. Bach [a], C. Lambrot [b], L. Augusto [b], M. Buée [a], S. Uroz [a,c]

Authors' affiliation

[a] Université de Lorraine - INRAE, UMR1136 Interactions Arbres-Microorganismes, Centre INRAE grand Est de Nancy, F-54280 Champenoux, France

[b] INRAE, Bordeaux Sciences Agro, UMR 1391 Interactions Sol Plante Atmosphère (ISPA), 33140 Villenave d'Ornon, France

[c] INRAE UR1138 Biogéochimie des Ecosystémes Forestiers, Centre INRA grand Est de Nancy, F-54280 Champenoux, France

Corresponding author: Sophie Mieszkin; sophie.mieszkin@univ-brest.fr

Running title: Sapwood and heartwood select different bacterial communities

Keywords

Oak decaying wood; bacteria; sapwood; heartwood; functional and metabolic potential; taxonomic diversity

*Current adress: Laboratoire de Microbiologie des Environnements Extrêmes LM2E, Univ Brest, CNRS, Ifremer, UMR 6197, IUEM, Rue Dumont d'Urville, F-29280 Plouzané, France

Abstract

Wood decay is an important process in forest ecosystems, which relies on wood chemical properties and the action of a complex community of decomposers. While the important role of fungi in this process is recognized, our knowledge concerning the colonization of decaying wood by bacteria, their relative distribution as well as their potential functional roles remain under-investigated. In this context, our aim was to characterize how the bacterial communities are structured at both taxonomic and functional levels along the soil-wood continuum, using oak discs positioned on the forest floor for nine months. Using a combination of culture-dependent and -independent methods associated to a physical measure of wood decay, we evidenced that at the middle stage of decay investigated, the heartwood- and sapwood-inhabiting bacterial communities significantly differed from one another in term of richness and taxonomic composition, but also from those of the bulk soil. The functional screening revealed low metabolic potentials and a higher frequency of cellulose decomposing bacteria in wood than in the bulk soil, suggesting an adaptation of these communities to this habitat and to the physical-chemical conditions occurring in decaying wood. Together, our data evidence that the colonization of decaying wood by bacteria is based on a deterministic process linking extrinsic and intrinsic factors.

1. Introduction

Forest ecosystems, due to the large area they cover on earth (up to 31% of land area in 2015), provide major ecosystem services. One of the most important is their capacity to stock carbon (C) and to act as a C sink (Pan et al., 2011; Seidl et al., 2014). In addition, trees accumulate inorganic nutrients taken from the soil in their biomass. Even if a significant C fraction is directly transferred to the surrounding environment through belowground allocation and root exudation (Litton et al., 2004; Hobbie, 2006), a major transfer comes from the seasonal litter deposition and after the death of trees or harvesting, during the wood decay. Consequently, decaying wood strongly impacts nutrient cycling and plays an important role in term of organic and inorganic nutrients recycling (Augusto et al., 2015; Ricker et al., 2016). In temperate regions, woody debris can be represented by logs, stumps or fine branches and can reach 2-65 m^3 ha^{-1} in managed forests where wood is harvested, while it can reach up to 1200 m^3 ha^{-1} in non-managed forests (Hahn and Christensen, 2005; Stokland et al., 2012). This material is a specific habitat for various organisms, such as insects and fungi, providing them an important source of cellulose, lignin and hemicellulose (Stokland et al., 2012; Seibold et al., 2015; Baldrian, 2017). However, the nutrients entrapped in the wood structure are not directly accessible to the wood biota, due to the recalcitrance of wood to decomposition. Indeed, the high content of lignin and the low nutrient content (mainly nitrogen (N) and phosphorus (P)) are not favorable to microbial development (Meerts, 2002). In addition, presence of toxic wood extractives and low pH conditions prevent wood microbial decomposition. All these parameters vary according to the wood species and the stage of decay, with some wood easily degradable (e.g. *Acer* sp. or *Tilia* sp.) and other more recalcitrant (i.e., *Quercus* sp. or *Acacia* sp.) (Weedon

et al., 2009; Rajala et al., 2012; Augusto et al., 2015).

A large body of literature suggests that fungi but also insects are the main decomposers of decaying wood. Insects, due to their capability of altering wood structure by tunneling and fragmentation and of decomposing wood through enzymatic digestion, are important engineers of early stage decay (Baldrian et al., 2016; Ulyshen, 2016). Fungi are well known for their ability to produce a large panel of extracellular lignocellulolityc enzymes to decompose the lignin and then the cellulose (Schneider et al., 2012; Mathieu et al., 2013; Baldrian et al., 2016; Noll et al., 2016). In comparison, less attention has been paid to wood-inhabiting bacteria, while they are known to colonize wood since the early steps of decomposition (Clausen, 1996; Blanchette, 2000; Kielak et al., 2016). Based on the analysis of the bacterial communities occurring at different stages of decomposition of pine-wood, Kielak et al. (2016) proposed that bacterial community assembly may be the result of a stochastic process at the initial stages of dead wood decomposition, and on the contrary determined by the wood properties at advanced stages. It was also reported that decaying bacteria communities could be diverse, potentially active at decomposing dead wood and capable of interacting with fungi (Valášková et al., 2009; Hervé et al., 2016; Johnston et al., 2016; Baldrian, 2017). Among the different studies performed on these communities, a dominance of *Proteobacteria*, *Actinobacteria*, *Bacteroidetes* and *Acidobacteria* was reported, suggesting an adaptation to the wood environment (Valášková et al., 2009; Hervé et al., 2014; Sun et al., 2014; Kielak et al., 2016; Rinta-Kanto et al., 2016). Noticeably, some bacterial classes or even genera were shown to differ according to the tree species (Prewitt et al., 2014; Moll et al., 2018) and/or the stage of decay (Hoppe et al., 2015). The potential structuring effect of the wood compartments (heartwood (HW), the dead

94 inner part of wood; sapwood (SW), the living outermost part of wood) on the bacterial
95 communities was also investigated, but such studies remain scarce (Zhang et al.,
96 2008; Moll et al., 2018). However, most of these studies described the community
97 composition, while the relative role of the bacterial communities in the decomposition
98 of wood is still largely underexplored.

99 Most of the current knowledge on the ability of bacteria to decompose wood
100 comes from the analysis of soil bacteria and on their capacities to hydrolyse cellulose
101 (Nicolitch et al., 2017), hemicelluloses (Lee et al., 2010), lignin (Větrovský et al.,
102 2014) or even pectin (Clausen, 1996). For instance, these functional abilities were
103 found in culturable representatives of *Acidobacteria* (*Silvibacterium bohemicum*)
104 (Lladó et al., 2016), of *Actinobacteria* (*e.g. Streptomyces*) (Nicolitch et al., 2016) or of
105 *Proteobacteria* (e.g., *Burkholderia*) (Hervé et al., 2016). Together, these results
106 suggest that the soil may act as a reservoir of bacteria capable of adapting to woody
107 debris and of participating to wood decomposition. Comparatively, few functional
108 analyses have been done on bacteria directly collected *in situ* from decaying wood
109 (Murray and Woodward, 2007; Valášková et al., 2009; Vorob'ev et al., 2009).
110 Consequently, determining whether bacteria are functionally structured according to
111 the stage of wood decay, the wood compartment or according to the tree species are
112 questions of importance in microbial ecology. As bacteria are not considered as the
113 main actors of wood decay in the early stages of decomposition, we investigated the
114 taxonomic and functional distribution of the bacterial communities at middle stage of
115 wood decay and across a soil-wood continuum. At this stage of decay, we
116 hypothesized that i) the direct role and the structure of the bacterial communities vary
117 according to the compartments (*i.e.*, bulk soil (BS) *versus* HW *versus* SW), and ii) the
118 two main wood compartments (HW and SW) select different bacterial communities

119 according to their own properties (i.e., nutritive content, wood biopolymers). To test
120 these hypotheses, we combined metabolic and functional bioassays, with a culture-
121 independent approach on oak wood samples incubated nine months on a forest floor.
122

123 ## 2. Materials and Methods

124 ### *2.1. Experimental site and sampling description*

125 The present study was performed in the forest experimental site of Champenoux
126 (north-eastern of France; Lat: 48.718°; Long: 6.347°; Alt: 248 m; 0.5 ha of surface).
127 The site is characterized as an oak forest aged of 110 years old where *Quercus*
128 *petraea* (*Q. petraea*) and *Carpinus betulus* represent the dominant tree species,
129 followed by some *Fagus sylvatica* and *Quercus robur* trees. The soil is classified as
130 an acidic luvic cambisol (pH-H_2O = 4.6 in the A1 horizon, 0-5 cm) and is
131 characterized by a mull-type humus and a loamy texture. The site is flat with
132 understory vegetation (*i.e.* oak and hornbeam seedlings, *Convallaria majalis* L.,
133 *Deschampsia cespitosa* L.).

134 At this site, four living oak trees of similar age (ca. 110 years old; 42 cm
135 diameter), spatially distant from 5 to 20 m, were selected. Oak was selected, as it
136 represents a major tree species in Europe and its coverage is expected to increase
137 with changes in temperatures and precipitations due to climate change (Hanewinkel
138 et al., 2013). An area of 25 m^2 (~5 m x ~5 m) was delimited around each oak tree,
139 and the litter was removed. Then, twenty oak discs were placed around each oak
140 tree directly on the surface of the soil and spatially separated from one another by a
141 distance of approximately 50 cm, giving a total of 80 wood discs. The wood discs
142 came from a sessile oak tree (*Q. petraea*) aged of approximately 48 years and cut off
143 in January 2015 from a neighboring forest plot and then stored and air-dried in the

144 laboratory protected from light and moisture for six months. Their average diameter
145 without the bark was 14.5 cm and their average thickness 2 cm. They were placed
146 directly in contact with the soil and incubated nine months in natural conditions to
147 enable wood decomposition (Fig. SI-1).

148 After a nine months incubation period, sampling was performed (April 2016) to
149 focus on the middle stage of wood decay and on the associated bacterial
150 communities. For each tree area and each oak disc, SW and HW as well as the soil
151 (BS) in contact with the wood discs were sampled. SW and HW samples were
152 recovered by drilling using a sterilized 10-mm drill bit. For each tree area, the
153 sawdust of the twenty oak discs was recovered from the two wood compartments
154 (HW and SW). The samples were then pooled to obtain four composite HW sawdust
155 samples (*n=20* per composite samples) and four composite SW sawdust samples
156 (*n=20* per composite samples). To compare the wood-inhabiting bacterial community
157 structures and functions, with those of the adjacent soil, 5 g of BS samples
158 underlying each wood-decaying disc (5 cm depth corresponding to the A1 horizon)
159 were sampled. The BS samples were then pooled for each tree area, leading to four
160 composite BS samples (*n=20* per composite samples). Each sample was stored in
161 sterile containers and once at the laboratory directly analyzed.

162 ***2.2. Soil chemical analyses***

163 For each replicate tree area, the chemical properties of the four BS samples have
164 been determined. Total N and C contents, both obtained after combustion at 1000°C,
165 and P content, were determined according to methods published by Olsen (1954),
166 Duchaufour and Bonneau, (1959) and Duval, (1963). The cation exchange capacity
167 (CEC) was determined according to the cobalti-hexamine method, which is based on
168 the titration of the cobalti-hexamine chloride soil extract. Exchangeable cations (Ca,

169 Mg, Na, K, Fe, Mn and Al) and protons were extracted using cobaltihexamine and
170 determined by inductively coupled plasma spectrometry-atomic emission
171 spectrometry (ICP-AES) for cations and by potentiometric measurement using 0.05
172 M KOH for protons. The pH was determined by the water method using a soil/water
173 ratio of 1:5 (w/v).

174 ***2.3. Wood decaying stage and chemical analyses***

175 The variation of density of the SW and HW was assessed during the wood decay
176 directly on specific oak discs incubated on the experimental site. For each replicate
177 tree area, one oak disk at T0 and five oak disks at T3, T6 and T9 months were
178 considered. A Pilodyn penetrometer with a 3 mm pin was used to measure
179 penetration depth (i*.e.,* the density) (Mäkipää and Linkosalo, 2011; Fundova et al.,
180 2018). For each sampling time and oak disc, three measures were performed for
181 both the SW and HW samples. Results were expressed as a mean percentage of
182 penetration depth for each wood compartment at each time point.

183 For each tree area and each wood compartment, the chemical properties of the
184 samples have been determined (four SW and four HW sawdust samples). All the
185 samples were dried at 65°C during 72h, homogenized and then sub-sampled for the
186 different analyses described in the supplementary section. Briefly, C and N were
187 analyzed through total combustion. Nutrients (*i.e.*, P, K, Ca, and Mg) were analyzed
188 after wet mineralisation. Quantification of the cellulose was obtained by successive
189 separations with different solvents using a Soxhlet extractor. Quantification of the
190 lignin content in the wood samples was performed with the Klason method. Finally,
191 the pH was determined for each sample.

192 ***2.4. Collection of bacterial strains***

For each sample (four BS, four SW and four HW), 1 g of sawdust (SW or HW) or BS was added to 20 mL of sterile distilled water and vortexed three times during 90 s. After a serial dilution in sterile distilled water, a volume of 0.1 mL from the dilutions 10^{-2} to 10^{-5}, was then spread in triplicate onto 1/10 diluted Tryptic Soy Agar (TSA) medium (Triptic Soy Broth (TSB) from Difco, 3 $g.L^{-1}$ and agar 15 $g.L^{-1}$) containing cycloheximide (100 $\mu g.L^{-1}$, final concentration). The pH of the medium was adjusted at 5 to fit with the pH found in oak sawdust and soil. All plates were then incubated at 25°C for 5 days. After incubation, the number of colony-forming units (CFU).g^{-1} from sawdust or soil samples was determined using the appropriate dilutions (10^{-3} and 10^{-4} according to the sample considered) permitting to quantify the densities of culturable bacteria in each compartment. For each compartment (BS, HW and SW) and replicate, and considering the dilution giving a total of 30 colonies per Petri dish, all the bacterial colonies were recovered. Bacterial isolates were then purified by three successive platings on 1/10 diluted TSA at pH 5 to obtain pure cultures. All the bacterial isolates were cryopreserved at -80°C in 35% glycerol. The bacterial collection was composed of 308 bacterial isolates that were distributed as follow: 117 BS isolates, 107 SW isolates and 84 HW isolates.

2.5. Metabolic and functional bioassays performed on bacterial isolates

The metabolic potential of each bacterial isolate was determined using Biolog microplates, which contain ninety-five different C sources. The GN2 microplates were selected in our study because they contain relevant substrates related to wood derivatives (ie, cellulose) or fungal metabolites (trehalose). The screening was performed according to the manufacturer's instruction. After 48 h incubation at 25°C, the absorbance was measured at 595 nm using an iMark microplate reader (Bio-Rad, USA) (see supplementary section for detailed information).

The capacity of each bacterial isolate to degrade organic matter and specific compounds found in wood (cellulose, lignin, xylan and chitin) as well as their ability to recover iron through the production of siderophores was evaluated. Five different bioassays allowing to measure: i) their cellulolytic ability (carboxy-methyl-cellulose (CMC) assay), ii) their lignolytic ability (Remazol brillant blue R (RBBR) assay), iii) their xylanolytic ability (xylan assay); iv) their chitinolytic ability (chitin assay) and v) their ability to mobilise iron (the CAS (chromoazurol-S assay), were used. Each bioassay is based on a gelosed medium allowing the measure of a discoloration halo. When compatible with the bioassay, the pH of the medium was adjusted to 5 to stay close to the pH of the wood and the soil. Composition of each medium and the experimental procedure are fully described in the supplementary section.

2.6. Molecular identification of bacterial strains and phylogenetic analyses

A fragment of the 16S rRNA gene was amplified using the universal set of primers pA and 907r (Edwards et al., 1989; Lane, 1991). The polymerase chain reaction (PCR) was performed in a total reaction volume of 50 µL containing 20 µL of master mix (PCR Taq PCR Master Mix, Qiagen), 2 µL of each primer (10 µM) and 2 µL of bacterial cells inoculum. PCR conditions were the following: 94°C for 4 min, then 30 cycles of 30 s denaturation at 94°C, 60 s annealing at 53°C, 90 s extension at 72°C, and a final extension step of 10 min at 72°C. PCR products were then purified using the QIAquick PCR purification kit (Qiagen) and concentration determined using a Nanodrop-1000 spectrometer (NanoDrop Technologies, Wilmington, DE, USA). The Sanger sequencing reactions were performed by MWG Eurofin Operon (Ebersberg, Germany) using the primer 907r. All the sequences were identified using the nucleotide BLAST program (Altschul, 1997). Sequence alignment and distance tree

were constructed using SeaView (version 4.7) (Gouy et al., 2010) and by using neighbor-joining algorithms with the Kimura two-parameter correction. Distance trees were constructed and bootstrap values were obtained using 1,000 replicates. Trees were generated using the Dendroscope 3 software (version 3.6.3) (Huson and Scornavacca, 2012).

The 16S rRNA Sanger sequences generated for this study were submitted to the Genbank database of NCBI under the accession numbers MN193104 - MN193411.

2.7. Illumina 16S high-throughput sequencing and data processing

Total DNA was extracted from 0.2 g of soil or oak sawdust (SW and HW) using the Fast DNA SPIN kit for soil extraction kit (MPbiomedical, Illkirch, France) following manufacturer's instructions with slight modifications including a step to grind the samples using a Retsch MM301 mixer (Retsch GbmH, Haan, Germany) and three additional washings with guanidine thiocyanate (5.5 M, pH 7) before to add the binding matrix. This step allows to efficiently denature endogenous nucleases and would facilitate the separation of proteins from the related sugars or polyols (Cox, 1968; Mason et al., 2003). To prepare the amplicon libraries for the paired-end Illumina sequencing, the primers 515f and 806r targeting the V4 region have been used (Caporaso et al., 2011). The sample multiplexing, the paired-end Illumina sequencing using 2x250 bp Miseq v3 and the de-multiplexing of the sequences were performed at GeT-PlaGe (Genotoul, Toulouse, France) according to the manufacturer's instructions.

Raw sequences processing was performed using FROGS (Find Rapidly OTU with Galaxy Solution) pipeline (Escudié et al., 2018). Paired sequences were merged into contigs with flash (Magoc and Salzberg, 2011), cleaned with cutadapt (Martin, 2011) and chimeras were removed with VSEARCH (Rognes et al., 2016). The clustering to

generate Operational Taxonomic Units (OTU) was then performed with SWARM algorithm (Mahé et al., 2014) using a local clustering threshold (97% similarity) and the taxonomic affiliation of each OTU was based on the reference databases NCBI Blast+ on SILVA123 16S (Camacho et al., 2009, Quast et al., 2013). Finally, a table presenting the number of 16S rRNA sequences assigned to each OTU as well as their taxonomic affiliation was generated. OTUs belonging to *Eukaryota* or *Archaea*, chloroplasts or mitochondria were discarded as well as contaminant OTUs generated by the extraction and amplification steps. All the singletons were removed for the OTUs analyses. Finally, the number of sequences per sample ranged from 17,806 to 39,132 giving a total of 334,380 sequences and 3,079 OTUs. OTU analyses were then performed using packages in R with a random subsampling to normalize each sample with the smallest number of sequences. The bacterial richness and alpha-diversity (Chao1, ACE, Shannon and inverse Simpson indexes) were calculated based on OTU relative abundance. The Illumina 16S rRNA sequences generated for this study were submitted to the Sequence Read Archive (SRA) of NCBI under the accession number PRJNA55031.

To determine both sequence homology and the relative environmental representativeness of the bacterial isolates recovered in our study, the Sanger 16S rRNA gene sequences were compared to the Illumina 16S rRNA gene sequences using the Basic Local Alignment Search Tool (BLAST) algorithm (Altschul et al., 1990). The Illumina 16S rRNA gene sequences of each compartment were used as database and an alignment of the Sanger 16S rRNA gene sequences was performed with NCBI-Blast+ using an e-value cutoff of 1 e-5. This analysis was done on the 253 bp overlapping between the Sanger and Illumina 16S rRNA gene sequences.

2.8. Statistical analyses

All statistical analyses were performed using R 3.2.3 software (R Core Team, 2015). The effect of the compartment (i.e., BS vs HW vs SW) was tested on the chemistry data and the bioassay data using an analysis of variance (one-way ANOVA, *P<0.05*), followed by a Tukey test. Wood density differences between the two oak wood compartments (SW and HW) was determined by a t-test. For the culture-dependent approaches, a Chi^2 test *(P<0.05*) analysis was performed to determine whether the frequency of distribution of the bacterial isolates according to their efficacy depended on their ecological origin.

For the Illumina 16S rRNA gene sequences and the related OTUs, the analyses were performed using R packages: phyloseq (McMurdie and Holmes, 2013), ape (Paradis et al., 2004) and vegan (Oksanen et al., 2007). The data were visualized using ggplot 2 (Wickham, 2009). The distribution of the bacterial communities according to their compartments was analyzed by performing multidimensional scaling (MDS) ordination using Bray Curtis matrix distance. Permutational multivariate analysis of variance (PERMANOVA) based on Bray-Curtis distances with 999 permutations were performed on the OTU table using the vegan package and the Adonis command. Analysis of variance and subsequent post-hoc Tukey's tests to compare taxonomic and functional differences between the compartments were also performed. Relative abundance values at all taxonomic levels (phylum, class, order, family, genus, OTU) were compared for taxa or OTUs presenting a minimum of 100 sequences. These values were transformed using the arcsine square root to achieve a normal distribution. When required, a p adjustment was done using the false-Discovery-Procedure (FDR) of Benjamini and Hochberg (1995) to determine the p-value threshold. Correlations between the major wood phyla and wood chemistry was assessed using Pearson correlations (*P<0.05*).

3. Results

3.1. Chemical analyses and wood decay stage assessment

The chemical analyses were done after nine months of incubation on the BS and wood samples (SW and HW sawdust) (Table SI-1A, B). The analysis of the pH revealed that BS harbored similar pH to the SW. The C/N ratio was 10 to 26 times lower in BS than in the wood compartments (Tab. SI-1A, B). The comparison of the wood compartments revealed that SW was characterized by significantly higher pH (pH-SW=4.63 *vs* pH-HW=3.75), higher amounts of N, P and Mg (ANOVA, $P<0.05$) and lower (approximately two times) C/N ratio (ANOVA, $P<0.05$). The content of cellulose and lignin (expressed on percentage relative to the global composition) appeared similar in HW and SW (ANOVA, $P>0.05$) (Tab. SI-1A).

After nine months of *in situ* decay, the visual inspection showed a strong fungal colonization of the SW compartment, while the HW compartment appeared poorly colonized (Fig. 1A, B). Significant variations of the wood density were observed based on the pilodyn measurements. Indeed, the penetration increased from T0 (25.8% ± 7.4 depth penetration in SW *vs* 16.4% ± 3.2 in HW) to T9 months (55.8% ± 12.6 in SW *vs* 30.4% ± 4.5 in HW). A significantly higher decay stage was measured for SW from T3 to T9 months compared to HW (t-Test; $P<0.05$) (Fig. 1C). According to these data, the decay stage of the oak discs after nine months of decay was considered as a middle stage.

3.2. OTUs distribution and diversity indices in soil and decaying wood

From the 213,672 16SrRNA sequences retained after bioinformatics treatments (Tab. SI-2), a total of 2,901 OTUs were generated. Comparison between the compartments revealed that the BS harbors significantly more OTUs (1,141 ± 189)

than the wood compartments (SW: 548 ± 127 and HW: 351 ± 123) (ANOVA, *P<0.05*). No difference was observed between the SW and HW (ANOVA, *P>0.05*) (Tab. SI-3). Among the total number of OTUs obtained, 9.8% were shared between the three compartments, while some were compartment specific (BS: 50.2%; SW: 14.3% and HW: 7.7% OTUs). Furthermore, 7.4% of the OTUs were shared between the two wood compartments and ca 5% of the OTUs were shared between BS and the wood compartments (Fig. SI-2). The observed (i.e., number of OTU observed) and the estimated richness (*i.e.,* chao1, ACE) as well as the alpha-diversity (i.e., Shannon, Inv. Simpson) were significantly higher in BS compared to the wood compartments (ANOVA, *P<0.05*). These indices tended to be higher in the SW than in the HW, but only significantly for the Shannon values (Tab. SI-3). Most of the OTUs obtained were assigned at the phylum (99.8%-23 different phyla) to family (88.1%) level, but only 66.4% of these sequences were assigned at the genus level. A global description of the taxonomic affiliation of these OTUs is presented in the table SI-4.

3.3. Structure and taxonomic composition of the bacterial communities in soil and decaying wood.

The properties of the different compartments considered (BS, SW and HW) strongly determined the bacterial community structure (*i.e.*, BS *vs* HW *vs* SW; F=10.6; R^2=0.70; *P*=0.01; PERMANOVA and Fig. 2A). Noticeably, the bacterial community structure significantly differed between SW and HW (*i.e.*, F=3.17; R^2= 0.35; *P=0.03;* PERMANOVA). A MDS analysis done on the OTUs confirmed this compartment effect (Fig. 2A, B). A detailed analysis of the taxonomic composition revealed that the wood-inhabiting bacterial community was significantly dominated by the *Proteobacteria* (59 to 73.4% of the 16S rRNA sequences in SW and HW,

368 respectively) compared to the BS compartment (ANOVA, *P<0.05*) (Fig. 2A, Tab. SI-
369 5). *Alphaproteobacteria* was the most abundant class in wood with 28.8% in SW and
370 41.7% in HW. A similar trend was observed for *Betaproteobacteria* (wood > BS;
371 ANOVA, *P*<0.05). Notably, our analyses revealed that the SW was significantly
372 enriched in *Bacteroidetes* (ANOVA, *P<0.05*). In contrast, the BS bacterial community
373 was mainly represented by *Acidobacteria*, followed by *Proteobacteria* (with
374 *Alphaproteobacteria* being the most represented class) and *Verrucomicrobia*
375 (12.8%). The relative abundance of *Acidobacteria* and *Verrucomicrobia* was
376 significantly higher in BS than in HW and SW (ANOVA, *P<0.05*). Noticeably, the
377 relative abundance of the *Bacteroidetes* (mainly present in SW) was positively
378 correlated with wood pH (*P=0.01*) and P concentration (*P=0.02*), while it was
379 negatively correlated with the C/N ratio (*P=0.02*). At the opposite, the relative
380 abundance of the *Alphaproteobacteria* (dominant in HW) was positively correlated
381 with the C/N ratio (*P=0.001*) but negatively correlated with P concentrations (*P=0.02*)
382 and the total amount of N (*P=0.02*) (Fig. SI-3).
383 Differences, at the OTUs level, between wood compartments and between wood
384 and BS were also observed. Dominant and specific OTUs of each compartment are
385 presented in Fig. 3, Table SI-6 and 7.

386 ### *3.4. Taxonomic affiliation of the bacterial isolates and relationship with*
387 ### *their ecological origin*

388 The quantification of the culturable bacteria by dilution-plating revealed that BS
389 harbored significantly higher densities (9.03 ± 0.14 Log_{10} CFU g^{-1} of soil) than the
390 SW (8.09 ± 0.08; ANOVA, *P<0.05*), but was not different from HW (8.80 ± 0.30;
391 ANOVA, *P>0.05*). HW harbored slightly higher densities than the SW (ANOVA,
392 *P<0.05*).

393 The taxonomic affiliation of the bacterial isolates revealed that most of them were
394 affiliated to *Proteobacteria* (77.7%), *Actinobacteria* (15.5%), *Acidobacteria* (4.5%)
395 and *Bacteroidetes* (2.3%). The relative distribution of the 30 genera detected is
396 presented in Figure 4 and Table SI-8. Notably, ca. 10% of the bacterial isolates had
397 less than 97% similarity with the 16S rRNA gene sequence of a known culturable
398 bacterial strain deposited in NCBI. Most of these particular isolates came from SW.

399 When the taxonomic affiliation of the bacterial isolates was linked to their
400 ecological niche (BS *vs* HW *vs* SW), our analysis showed that isolates belonging to
401 the *Beta*- and *Gammaproteobacteria* were common to the three compartments (Fig.
402 4; Tab. SI-8). However, we noticed that the SW compartment was significantly
403 enriched in *Gammaproteobacteria* isolates (SW, 57.8% of the isolates; BS, 24.4%
404 and HW, 17.8%; Chi^2, $P<0.002$), whereas, the BS compartment was significantly
405 enriched in *Betaproteobacteria* isolates (BS, 49.6% of the isolates; SW, 30.6% and
406 HW, 19.8%; Chi^2, $P<0.003$). Interestingly, all the isolates belonging to *Acidobacteria*
407 and *Bacteroidetes* (*Alphaproteobacteria*) were exclusively found in wood (SW and/or
408 HW). Several genera were strongly represented and only detected in wood. This is
409 the case of *Sphingomonas*, *Mucilaginibacter* and *Luteibacter* in SW, and *Acidocella,*
410 *Acidipila* and *Novosphingobium* in HW. At the opposite, *Actinobacteria* strains
411 assigned to *Streptomyces*, *Kitasatospora*, *Arthrobacter* and *Streptacidiphilus* were
412 dominant in BS. Strains assigned to the *Paraburkholderia* and *Dyella* genus were
413 recovered in the three compartments considered, with *Paraburkholderia* representing
414 34.7% of the total of the isolates.

415 ***3.5. Metabolic and functional potentials of the culturable bacterial***
416 ***communities***

The metabolic bioassays based on Biolog plates revealed that the BS bacterial isolates harbored significantly higher metabolic potentials than those of the decaying-wood compartments (BS>SW=HW) (ANOVA; *P<0.05*) (Fig. SI-4). Such difference was observed at both substrate and substrate category levels (Fig. SI-4 and Fig 5). Comparisons between wood bacterial isolates showed that HW isolates had a higher metabolic potentials for substrates belonging to (i) the carboxylic acid group (ca. 2 fold higher than SW for quinic acid, sebacic acid, succinamic acid, D-glucosaminic acid, glycyl-L-glutamic acid) (ii) the amino acid group (ca. 2 fold higher than SW for L-histidine); (iii) the miscellaneous group (15 fold higher than SW for thymidine); and finally, (iv) the amine-amide group (aminoethanol, 3 fold higher). Beta-methyl-D-glucoside was almost the unique substrate more effectively metabolized by the SW bacterial isolates (4 fold higher than HW isolates) (Fig. 5).

Among the functional bioassays performed, the cellulose decomposition assay gave the highest number of positive bacterial isolates. Indeed, ca. 12.6% of the bacterial isolates tested appeared capable of degrading cellulose (Fig. SI-5). Significantly more bacteria isolated from HW (ca. 28.6%) were capable of degrading cellulose, than those coming from SW (13.4%) and BS (10.3%) (Chi2; *P<0.0001*). In term of effectiveness, the BS and HW bacterial isolates tended to be more effective at degrading cellulose (halo diameters: 0.21cm±0.04 for BS isolates and 0.20cm±0.02 for HW isolates) than the SW isolates (0.12cm±0.02; ANOVA 443 *P=0.07*). In the wood compartments, the ability to degrade cellulose was mainly encountered for bacterial isolates assigned to the genus *Mucilaginibacter* (relative efficacy to degrade cellulose (halo diameter): 0.81cm±0.51), *Novosphingobium* (0.50cm±0.51) and *Acidisoma* (0.48cm±0.41). Noticeably, 71.4% of the *Mucilaginibacter* isolates were capable of hydrolyzing cellulose, while only 54.5% for

442 *Acidisoma* and 38.5% for *Novosphingobium* (Fig. 6). In contrast, in the BS
443 compartment this function was mainly encountered for bacterial isolates assigned to
444 the genus *Kitasatospora* (2.05cm±1.61) and *Streptomyces* (0.73cm±1.21) (Fig. 6).
445 Concerning the ability to degrade chitin, only 8.5% of the bacterial isolates were
446 capable of degrading this compound and were mainly isolated from BS (45.5% of the
447 isolates capable to hydrolyze chitin were originated from BS) (Fig. SI-5). The BS and
448 HW bacterial isolates tended to be more effective at degrading chitin. The bacterial
449 genera presenting the highest potential were assigned to the genus *Collimonas* (halo
450 diameter: 1.83cm±0.49; only recovered from the BS compartment), *Luteibacter*
451 (0.91±0.74; only recovered from the HW compartment) and *Streptomyces*
452 (0.62cm±0.72; only recovered from the BS compartment). While all of the *Collimonas*
453 isolates were effective at hydrolyzing chitin, only 57.1% and 25% of the *Luteibacter*
454 and *Streptomyces* isolates did it (Fig. 6).
455 For the other functions related to organic matter decomposition, the ability to
456 degrade xylan was only detected for seven bacterial isolates (2.8% of the bacterial
457 collection) (Fig. 6) and none of the bacterial isolates was capable of degrading lignin.
458 Concerning the ability to mobilize iron, ca. 24% of the bacterial isolates tested were
459 positives (Fig. SI-5). Significantly higher proportions were observed in BS (72.9% of
460 the isolates mobilizing iron) than in HW (18.6%) or SW (8.5%) (Chi^2; *P<0.001*). The
461 bacterial genera presenting the highest potentials to mobilize iron were assigned to
462 the genus *Pseudomonas* (relative efficacy to mobilize iron (halo diameter):
463 2.08cm±0.98) and in a lesser extend to *Collimonas* isolates (1.48cm±0.69) with
464 respectively 85.7% and 100% of the isolates of these genera being effective for iron
465 mobilization. The two other genera: *Paraburkholderia* (0.7cm±0.93) and

Streptomyces (0.2cm±0.49) were significantly less efficient than *Pseudomonas* isolates (ANOVA, *P<0.05*) (Fig.6).

3.6. Comparison of the Sanger and Illumina 16S RNA gene sequences

This analysis highlighted that all the 308 bacterial isolates of our collection had a minimum of 97% of sequence homology with at least one OTU of the Illumina sequence dataset. When the highest homology was considered, this analysis revealed that the bacterial isolates corresponded to 65 OTUs identified in the Illumina dataset. These OTUs represented 55.4% of the total number of Illumina 16S rRNA sequences. Interestingly, the most represented bacterial isolates in our collection (at the genus level) were also among the dominant in the OTUs (Rank in the collection / rank in the OTU table; *Paraburkholderia* (1/1), *Acidisoma* (2/5), *Dyella* (3/12), *Acidocella* (6/4) and more distantly *Pseudomonas* (7/114) (data not shown).

4. Discussion

To date, a few studies have investigated the taxonomic diversity and especially the metabolic and functional role of decaying wood-inhabiting bacteria (Murray and Woodward 2007; Folman et al., 2008; Hervé et al., 2016). However, this aspect is of importance to better understand the decaying wood process and how bacteria contribute to the recycling of the nutritive elements accumulated in the tree biomass. Therefore, to investigate the structure and the potential role of the bacterial communities, we used oak discs installed on the floor of an oak forest site, mimicking partially in this way the conditions when trees fall on the soil and initiate a decomposition process. A combination of culture-dependent and -independent approaches combined with chemical analyses were used and comparisons with bulk soil bacteria was made to highlight the soil-decaying wood continuum.

4.1. Edaphic origin of decaying oak wood-inhabiting bacteria.

How decaying-wood is colonized by microorganisms is rather difficult to determine. Indeed, part of the microorganisms found in decaying wood may originate from the tree tissues (i.e., endophytes), atmospheric deposits or from the surrounding BS (Baldrian et al., 2016). Previous analyses provided clear evidences that whether or not an initial microbiota exists inside trees during their life, its biomass and diversity changed importantly and quickly between the early and later stages of wood decay (Tláskal et al., 2017). The Venn diagram analyses done in our study suggest that a part of the wood-inhabiting bacterial communities is also part of the BS bacterial communities (10.6%). The other OTUs only detected in wood may represent minor groups occurring in BS but not detected by sequencing or may be coming from other locations (i.e., atmosphere, endophytes of the oak discs, woody debris fallen on the oak discs). Interestingly, Probst et al. (2018) also observed that a significant part of the OTUs identified in decaying wood were shared with the surrounding BS, supporting an edaphic origin of wood-inhabiting bacteria. The detailed analysis of the culture-dependent approach also indicated that several bacterial genera were detected in both the BS and wood compartments including bacterial isolates assigned to *Paraburkholderia*, *Dyella* and *Pseudomonas*. These bacterial genera have frequently been described in forest soils, underlying their ability to adapt to various habitats such as decaying wood (Folman et al., 2008; Lladó et al., 2016; Nicolitch et al., 2017). Supporting this hypothesis, Hervé et al. (2014) demonstrated that *Burkholderia* and *Dyella* strains isolated from BS and inoculated in wood sawdust microcosms became dominant after a succession of enrichment steps. Those results support the idea that the BS in forest ecosystem represents a seedbank with a high diversity of functional groups capable of decomposing wood.

516 This is not surprising as the topsoil is continuously in contact with litter and wood
517 debris. Consequently, the abundance of wood-inhabiting bacteria depends on the
518 turnover of tree biomass (wood, litter) with bacteria returning to the surrounding soil
519 at the end of the wood decomposition process (Probst et al., 2018).

520 **4.2. Metabolic and functional potential of decaying oak wood-inhabiting**
521 **bacterial communities differ from soil bacterial communities.**

522 Decaying oak wood-inhabiting bacterial communities may directly or indirectly
523 contribute to wood decomposition. In this study, we tested the hypothesis of a direct
524 role of bacteria in wood decay. To do it, a functional screening targeting the main
525 wood constituents (cellulose, xylan and lignin) was performed. We also focused on
526 chitin because it is an essential constituent of fungal cell walls, and the
527 decomposition of the wood is characterized also by a dynamic succession of different
528 fungi during the whole process (Rajala et al., 2015), generating an important fungal
529 necromass potentially recyclable by bacteria. Mobilization of iron was also studied
530 because iron plays a role in the oxidative process of wood decomposition (Goodell et
531 al., 1997). Our results showed that cellulose degrading bacteria were more frequent
532 in wood, especially in HW, than in the surrounding BS. However, BS was
533 characterized by bacterial isolates presenting a higher effectiveness at degrading
534 cellulose, xylan or chitin or at mobilizing iron than HW and SW. These results differ
535 from those obtained by Hervé et al. (2016) where there was no functional difference
536 observed between bacteria isolated from BS and those adapted to beech decaying
537 wood. However, our experiment was done *in situ* and over a longer period, which
538 may explain the differences we observed. Looking at the taxonomic identity of the
539 strains, we found that representatives of the *Kitasatospora* genus, isolated from BS,
540 were among the most effective at degrading cellulose. Nonetheless, representatives

of the *Mucilaginibacter, Acidisoma* and *Novosphingobium* genera, all isolated from wood (SW and HW), were also effective. Except for *Novosphingobium,* these genera were previously identified as important cellulose decomposers (Štursová et al., 2012; Lladó et al., 2016; Lopez-Mondejar et al., 2016; Nicolitch et al., 2016). The absence of bacterial strains able to degrade lignin confirms the results obtained by Murray and Woodward (2007) and Hervé et al. (2016). Those results suggest that the ligninolytic activity is probably mainly attributable to fungi (Janusz et al. 2017). However, bacterial strains affiliated to the *Actinomycetes*, *Alphaproteobacteria* and *Gammaproteobacteria* have been reported for their ability to break down lignin (Bugg et al., 2011; Janusz et al., 2017). The metabolic assays (strain by strain) revealed significant differences between wood and soil bacteria. The decaying wood-inhabiting bacteria presented weaker metabolic potentials than the BS isolates, but a conserved ability to consume cellulose and hemicellulose derived monomers such as alpha D-glucose, D-mannitol, D-mannose, L-arabinose, N-acetyl-D-glucosamine, L-fucose, D-sorbitol, D-fructose, L-rhamnose and beta-methyl-D-glucoside. The preferential use of these wood monomers by bacterial strains isolated from a wood environment was also demonstrated by Hervé et al. (2016). Another hypothesis explaining the enrichment of particular bacteria in decaying wood is their indirect role in the wood decay process (Clausen 1996; Johnston et al., 2016). Indeed, it was proposed that wood-colonizing fungi enrich their habitat with bacteria capable of fixing nitrogen or providing them other services, promoting fungal development and wood decomposition. Although this hypothesis was not tested in our study, the chitin degradation assay performed evidenced that some HW bacteria may have a negative impact on fungi. Altogether, the results obtained through the functional bioassays suggest that the decaying wood-inhabiting bacteria are adapted to their

566 environment where substrates are less diverse than in the soil and potentially more
567 recalcitrant to decomposition.

568 **4.3 Wood properties determine the structure of the bacterial communities.**

569 Intrinsic (chemistry) and extrinsic (environment) factors may impact the
570 structuration of the wood-inhabiting bacterial communities. Indeed, wood is not a
571 homogenous material and it is established that HW and SW present different
572 properties. In our study, the chemical analyses done on the SW and HW
573 compartments clearly evidenced that SW presented significantly higher content of N,
574 P and Mg, and lower C/N ratio than HW. In addition, HW presented a significantly
575 more acidic pH than SW. Interestingly, C/N ratio and pH have been proposed as
576 driving factors governing the composition of the wood-inhabiting bacterial
577 communities (Folman et al., 2008; Hoppe et al., 2015). In this sense, the correlation
578 analyses done between the Illumina 16S rRNA sequences and the wood properties
579 revealed that the C/N ratio was negatively correlated with the abundance of
580 *Bacteroidetes*, while it was positively correlated with *Alphaproteobacteria*. In addition,
581 pH appeared positively correlated with the abundance of *Bacteroidetes*. These two
582 wood chemical properties were also reported as main drivers of bacterial community
583 structures in decaying wood (Tláskal et al., 2017; Moll et al., 2018). The HW
584 compartment is also known to present a higher phenolic extractives content (up to
585 10%), which may have an antimicrobial activity (Kebbi-Benkeder et al., 2015;
586 Miranda et al., 2017; Moll et al., 2018). The colonization of the wood compartments
587 by other types of decaying wood organisms (i.e., fungi and insects; Kubartova´ et al.,
588 2012; Ulyshen, 2016; Leonhardt et al., 2019) may also be important extrinsic factors
589 driving the structure of the bacterial communities. Indeed, fungi and insects are
590 known to be important wood decomposers (Baldrian et al., 2016; Ulyshen, 2016) and

591 their interactions with bacteria are known to have an important ecosystemic role
592 (Folman et al., 2008; Frey-Klett et al., 2011; Hervé et al., 2016; Johnston et al.,
593 2016). Notably, bacterial–fungal consortia were shown to degrade wood more
594 effectively than fungi alone (Murray and Woodward, 2003; Hervé et al., 2016). In our
595 study, a visual inspection of the oak discs at the end of the incubation revealed an
596 important fungal development (i.e., hyphae) on the surface of SW, which was not
597 visible on HW. Consequently, it is strongly plausible that differences between HW
598 and SW in term of bacterial community structure are also due to the presence of
599 fungal communities. Whether the density of culturable bacteria was similar between
600 the HW and BS, the taxonomic structuration differed. Although it was only significant
601 for the richness index (i.e., Shannon), all the richness and diversity indices tended to
602 have lower values for the HW compartment compared to SW. A similar trend was
603 obtained by Moll et al. (2018) considering 30 tree species, including oak tree. In our
604 study, the decrease of diversity and richness corresponded to higher abundances of
605 *Alpha-* and *Betaproteobacteria* and lower abundance of *Bacteroidetes* in HW than in
606 SW. These results differ from the study of Moll et al. (2018) where the major
607 difference between HW and SW of decaying oak wood relied on an increase of
608 *Acidobacteria* in SW. The culturable approach also permitted to differentiate the SW
609 and HW compartments. Notably, several genera were only isolated in HW (i.e.,
610 *Acidocella*) or only in SW (i.e., *Mucilaginibacter, Luteibacter, Yersinia*), evidencing a
611 relatively good overlap between the conclusions obtained by the culture-dependent
612 and -independent approaches. Together, these results highlight that specific bacterial
613 communities are enriched in each wood compartment, potentially according to the
614 wood properties as well as due to the interactions with the fungal communities
615 occurring in decaying wood.

5. Conclusion

Our study highlighted that at middle stage of decay, a significant part of the microbiota enriched in wood is shared with the surrounding bulk soil (BS), evidencing that decaying wood is not disconnected from its environment. At the same time, ca 30% of the OTUs identified in our study were only detected in the wood compartments, highlighting the enrichment of particular taxa and/or functional group in decaying wood. Interestingly, the bacterial communities occurring in the SW and HW compartments significantly differed in their taxonomic and functional compositions. The distribution of some taxa appeared significantly correlated to the wood chemical properties. This differentiation clearly evidences that the colonization of decaying wood by bacteria is based on a deterministic process linking extrinsic and intrinsic factors. Although the bacteria isolated from the wood compartments presented lower metabolic potentials compared to those of the surrounding BS, they were characterized by a conserved ability to decompose cellulose/hemicellulose and derivatives. In contrast, no bacteria capable of decomposing lignin was identified. Those results suggest that wood-inhabiting bacteria are capable of degrading the easily degradable part of wood, but that the decomposition of the recalcitrant part (i.e., lignin) is probably done by fungi (van der Wal et al., 2015; Hoppe et al., 2015; Leonhardt et al., 2019; Tláskal et al., 2017). Another hypothesis may be that these bacterial communities indirectly contribute to wood decay through the promotion of fungal growth, highlighting a possible functional complementation between bacteria and fungi (Frey-Klett et al., 2011). Future work will need to focus i) on the functional structuration of the bacterial communities at different stage of decay, ii) on bacterial-fungal interactions and/or co-occurrence studies during wood decay and iii) on the

641 indirect role of bacteria such as nitrogen fixation during wood decay. Combination of
642 field experiments and controlled microcosms will be necessary to better understand
643 the role of microbial interactions and community successions in wood decay.
644
645 **6. Acknowledgments**
646 This work was supported by the Laboratory of Excellence Arbre (ANR-11- LABX-
647 0002-01; DivBacto project) and by the EFABA project (SF 4242; AI-16-3). The
648 UMR1136 is supported by the French Agency through the Laboratory of Excellence
649 Arbre (ANR-11-LABX-0002-01). We would like also to thank A. Deveau for her help
650 concerning the analysis of the Illumina Miseq 16S rRNA sequences.
651
652 **7. Author contributions**
653 S.M., S.U. and M.B., conceived and designed the study; S.M., C.B., P.R. and
654 C.L., performed field and laboratory work; S.M. and S.U., analyzed the data and
655 wrote the paper. All authors reviewed and edited the manuscript.
656

Figure Legends:

Figure. 1. Evidence of the oak decay stage. A. Picture of a freshly cut oak disc at the beginning of the experiment (T0 month). **B.** Picture of an oak disc after 9 months of *in situ* decay (T9 months) showing the side in direct contact with the soil. **C.** Mean percentage of the penetration depth for the sapwood (SW) and heartwood (HW) compartments assessed using a Pilodyn penetrometer at T0 (*n=3*) and T3, T6 and T9 months (*n=20* per time point). Significant differences between the two wood compartments for each time point are presented using a star (*P<0.05* according to a t-test).

Figure 2. A. Relative abundance of the Illumina Miseq 16S rRNA sequences from bacterial taxonomic phyla for each compartment (oak decaying sapwood (SW) and heartwood (HW) and bulk soil (BS)). The ten most abundant phyla were considered. **B. Multidimensional scaling (MDS) ordination using Bray Curtis matrix distance representing the distribution of the bacterial communities according to each compartment (oak decaying sapwood (SW) and heartwood (HW) and bulk soil (BS)).**

Figure 3. Heatmap showing the relative abundance of the 10 most important OTUs per compartment (oak decaying sapwood (SW) or heartwood (HW) or bulk soil (BS)) expressed in percentage.

Figure 4. Neighbor-joining tree showing the phylogenetic relationships of bacterial isolates depending on their compartment (oak decaying sapwood (SW) and heartwood (HW), Bulk soil (BS)), based on PCR sequencing of a portion of the 16S rRNA gene. A bootstrap analysis was performed with 1000 repetitions. Due to the relatively large number of sequences analysed, we have chosen one representative sequence in each genus for the tree representation. Pie chart on the right side of each genus represents the distribution of bacterial isolates assigned to this genus according to their origin (blue: BS, red: SW, green: HW). Number accessions for reference strains from NCBI are indicated in brackets.

Figure 5. Heatmap analysis of the metabolic potentials obtained using Biolog GN2 microplates. A total of 304 bacterial isolates was tested. Detailed analysis of the substrates for which metabolic potentials varied significantly among the bacterial isolates depending on the compartment (oak decaying sapwood (SW) and heartwood (HW) and bulk soil (BS)) was done. Statistics on the right of the heatmap were obtained according to a one-way ANOVA followed by a Tukey test (NS: not significant, *$P<0.05$, **$P<0.01$, ***$P<0.001$).

Figure 6. Relationship between functional efficacy and taxonomic affiliation. For each bacterial genus represented by a minimum of three effective isolates, their

relative efficacy to hydrolyze cellulose, xylan and chitin and to mobilize iron is presented, whatever their compartment (oak decaying sapwood (SW) and heartwood (HW) and bulk soil (BS)) of the bacterial isolates. Lowercase letters (a, b, c, d or e) indicate significant differences between genus efficacies. Statistics were obtained according to a one-way ANOVA followed by a Tukey test ($P<0.05$). The number of isolates tested per genus as well as their repartition according to their comprtment (BS, SW or HW) is presented under the bars. The error bars indicate the standard error.

References

Altschul, S.F., 1997. Evaluating the statistical significance of multiple distinct local alignments. In Theoretical and Computational Methods in Genome Research, Springer, Boston, MA. 1-14.

Altschul, S.F., Madden, T.L., Schäffer, A.A., Zhang, J., Zhang, Z., Miller, W., Lipman, D.J., 1997. Gapped BLAST and PSI-BLAST: a new generation of protein database search programs. Nucleic Acids Research 25, 3389-3402.

Altschul, S.F., Gish, W., Miller, W., Myers, E.W., Lipman, D.J., 1990. Basic local alignment search tool. Journal of Molecular Biology 215, 403-410.

Augusto, L., De Schrijver, A., Vesterdal, L., Smolander, A., Prescott, C., Ranger, J., 2015. Influences of evergreen gymnosperm and deciduous angiosperm tree species on the functioning of temperate and boreal forests. Biological Reviews 90, 444-466.

Baldrian, P., 2017. Forest microbiome: diversity, complexity and dynamics. FEMS Microbiology Reviews 41, 109-130.

Baldrian P., Zrůstová, P., Tláskal, V., Davidová, A., Merhautová, V., Vrška. T., 2016. Fungi associated with decomposing deadwood in a natural beech-dominated forest. Fungal Ecology 23, 109-122.

Benjamini, Y., Hochberg, Y. 1995. Controlling the false discovery rate: a practical and powerful approach to multiple testing. Journal of the Royal statistical society: series B (Methodological), 57, 289-300.

Blanchette R.A., 2000. A review of microbial deterioration found in archaeological wood from different environments. International Biodeterioration and Biodegradation 46, 189-204.

Bugg, T.D., Ahmad, M., Hardiman, E.M., Singh, R., 2011. The emerging role for bacteria in lignin degradation and bio-product formation. Current Opinion in Chemical Biology 22, 394-400

Camacho, C., Coulouris, G., Avagyan, V., Ma, N., Papadopoulos, J., Bealer, K., Madden, T.L., 2009. BLAST+: architecture and applications. BMC Bioinformatics 10, 421.

Caporaso, J.G., Lauber, C.L., Walters, W.A., Berg-Lyons, D., Lozupone, C.A., Turnbaugh, P.J., *et al.*, 2011. Global patterns of 16S rRNA diversity at a depth of millions of sequences per sample. Proceedings of the National Academy of Sciences 108, 4516-4522.

Clausen, C.A., 1996. Bacterial associations with decaying wood: a review. International Biodeterioration and Biodegradation 37, 101-107.

Cox, R.A., 1968. The use of guanidinium chloride in the isolation of nucleic acids. In

Methods in enzymology, Academic Press 12, 120-129.

Duchaufour, P., Bonneau, M., 1959. Une nouvelle méthode de dosage du phosphore assimilable dans les sols forestiers. Bulletin AFES 4, 193-198.

Duval, L., 1963. Etude des conditions de validité du dosage céruléomolybdique de l'acide phosphorique. Conséquences Pratiques. Chimie Analytique 45, 237-240.

Edwards, U., Rogall, T., Blöcker, H., Emde, M., Böttger, E.C., 1989. Isolation and direct complete nucleotide determination of entire genes. Characterization of a gene coding for 16S ribosomal RNA. Nucleic Acids Research 17, 7843-7853.

Escudié, F., Auer, L., Bernard, M., Mariadassou, M., Cauquil, L., Vidal, K., Maman, S., Hernandez-Raquet, Guillerma, Combes, Sylvie., Pascal, G. 2018. FROGS: find, rapidly, OTUs with galaxy solution. Bioinformatics 34, 1287-1294.

Folman, L.B., Klein Gunnewiek, P.J., Boddy, L., De Boer, W., 2008. Impact of white-rot fungi on numbers and community composition of bacteria colonizing beech wood from forest soil. FEMS Microbiology Ecology 63, 181-191.

Frey-Klett, P., Burlinson, P., Deveau, A., Barret, M., Tarkka, M., Sarniguet, A., 2011. Bacterial-fungal interactions: hyphens between agricultural, clinical, environmental, and food microbiologists. Microbiology and Molecular Biology Reviews 75, 583-609.

Fundova, I., Funda, T. Wu, H.X., 2018. Non-destructive wood density assessment of Scots pine (*Pinus sylvestris* L.) using Resistograph and Pilodyn. PLoS one 13, e0204518.

Goodell, B., Jellison, J., Liu, J., Daniel, G., Paszczynski, A., Fekete, F., Krishnamurthy, S., Jun, L., Xu, G., 1997. Low molecular weight chelators and phenolic compounds isolated from wood decay fungi and their role in the fungal biodegradation of wood. Journal of Biotechnology, 53, 133-162.

Gouy, M., Guindon, S., Gascuel, O., 2010. SeaView version 4: a multiplatform graphical user interface for sequence alignment and phylogenetic tree building. Molecular Biology and Evolution 27, 221-224.

Hahn, K., Christensen, M., 2005. Dead wood in European forest reserves - a reference for forest management. In: Marchetti M (ed.). Monitoring and Indicators of Forest Biodiversity in Europe - From Ideas to Operationality. European Forest Institute 181-91.

Hanewinkel, M., Cullmann, D.A., Schelhaas, M.J., Nabuurs, G.J., Zimmermann, N.E., 2013. Climate change may cause severe loss in the economic value of European forest land. Nature Climate Change 3, 203-207.

Hervé, V., Le Roux, X., Uroz, S., Gelhaye, E., Frey-Klett, P., 2014. Diversity and structure of bacterial communities associated with *Phanerochaete chrysosporium* during wood decay. Environmental Microbiology 16, 2238-2252.

Hervé, V., Ketter, E., Pierrat, J.C., Gelhaye, E., Frey-Klett, P., 2016. Impact of *Phanerochaete chrysosporium* on the functional diversity of bacterial communities associated with decaying wood. PloS one 11, e0147100.

Hobbie, E.A., 2006. Carbon allocation to ectomycorrhizal fungi correlates with belowground allocation in culture studies. Ecology 87, 563-569.

Hoppe, B., Krüger, D., Kahl, T., Arnstadt, T., Buscot, F., Bauhus, J., Wubet, T., 2015. A pyrosequencing insight into sprawling bacterial diversity and community dynamics in decaying deadwood logs of *Fagus sylvatica* and *Picea abies*. Scientific Reports 5, 9456.

Huson, D.H., Scornavacca, C., 2012. Dendroscope 3: an interactive tool for rooted phylogenetic trees and networks. Systematic Biology 61, 1061-1067.

Janusz, G., Pawlik, A., Sulej, J., Świderska-Burek, U., Jarosz-Wilkołazka, A., Paszczyński, A., 2017. Lignin degradation: microorganisms, enzymes involved, genomes analysis and evolution. FEMS microbiology reviews 41, 941-962.

Johnston, S.R., Boddy, L., Weightman, A.J., 2016. Bacteria in decomposing wood and their interactions with wood-decay fungi. FEMS Microbiology Ecology 92, fiw179.

Kebbi-Benkeder, Z., Colin, F., Dumarçay, S., Gérardin, P., 2015. Quantification and characterization of knotwood extractives of 12 European softwood and hardwood species. Annals of Forest Sciences 72, 277-284.

Kielak, A.M., Scheublin, T.R., Mendes, L.W., Van Veen, J.A., Kuramae, E.E., 2016. Bacterial community succession in pine-wood decomposition. Frontiers in Microbiology 7, 231.

Kubartová, A., Ottosson, E., Dahlberg, A., Stenlid, J., 2012. Patterns of fungal communities among and within decaying logs revealed by 454 sequencing. Molecular Ecology 21, 4514-4532.

Lane, D.J., 1991. 16S/23S rRNA sequencing. Nucleic acid techniques in bacterial systematics 115-175.

Lee, C.S., Jung, Y.T., Park, S., Oh, T.K., Yoon, J.H., 2010. *Lysinibacillus xylanilyticus* sp. nov., a xylan-degrading bacterium isolated from forest humus. International Journal of Systematic and Evolutionary Microbiology 60, 281-286.

Leonhardt, S., Hoppe, B., Stengel, E., Noll, L., Moll, J., Bässler, C., Dahl, A., Buscot, F., Hofrichter, M., Kellner H., 2019. Molecular fungal community and its decomposition activity in sapwood and heartwood of 13 temperate European tree species. PLoS one 14, e0212120.

Litton, C.M., Ryan, M.G., Knight, D.H., 2004. Effects of tree density and stand age on carbon allocation patterns in postfire lodgepole pine. Ecological Applications 14, 460-475.

857 Lladó, S., Žifčáková, L., Větrovský, T., Eichlerová, I., Baldrian, P., 2016. Functional
858 screening of abundant bacteria from acidic forest soil indicates the metabolic
859 potential of Acidobacteria subdivision 1 for polysaccharide decomposition. Biology
860 and Fertility of Soils 52, 251-260.
861
862 Lopez-Mondejar, R., Zuhlke, D., Becher, D., Riedel, K., Baldrian, P., 2016. Cellulose
863 and hemicellulose decomposition by forest soil bacteria proceeds by the action of
864 structurally variable enzymatic systems. Scientific Reports 6, 25279.
865
866 Mahé, F., Rognes, T., Quince, C., de Vargas, C., Dunthorn, M., 2014. Swarm: robust
867 and fast clustering method for amplicon-based studies. PeerJ 2, e593.
868
869 Magoc, T., Salzberg, S.L., 2011. FLASH: fast length adjustment of short reads to
870 improve genome assemblies. Bioinformatics 27, 2957-2963.
871
872 Mäkipää, R., Linkosalo, T.**,** 2011. A non-destructive field method for measuring wood
873 density of decaying logs. Silva Fennica 45, 1135-1142.
874
875 Martin, M., 2011. Cutadapt removes adapter sequences from high-throughput
876 sequencing reads. European Molecular Biology network Journal 17, 10-12.
877
878 Mason, P.E., Neilson, G.W., Dempsey, C.E., Barnes, A.C., Cruickshank, J.M., 2003.
879 The hydration structure of guanidinium and thiocyanate ions: implications for protein
880 stability in aqueous solution. Proceedings of the National Academy of Sciences 100,
881 4557-4561.
882
883 Mathieu, Y., Gelhaye, E., Dumarçay, S., Gérardin, P., Harvengt, L., Buée, M., 2013.
884 Selection and validation of enzymatic activities as functional markers in wood
885 biotechnology and fungal ecology. Journal of Microbiological Methods 92, 157-163.
886
887 McMurdie, P.J., Holmes, S., 2013. phyloseq: An R package for reproducible
888 interactive analysis and graphics of microbiome census data. PLoS ONE 8, e61217.
889
890 Meerts, P. 2002. Mineral nutrient concentrations in sapwood and heartwood: a
891 literature review. Annals of Forest Science 59, 713-722.
892
893 Miranda, I., Sousa, V., Ferreira, J., Pereira, H., 2017. Chemical characterization and
894 extractives composition of heartwood and sapwood from *Quercus faginea*. PloS one
895 12**,** e0179268.
896
897 Moll, J., Kellner, H., Leonhardt, S., Stengel, E., Dahl, A., Bässler, C., Buscot, F.,
898 Hofrichter, M., Hoppe, B., 2018. Bacteria inhabiting deadwood of 13 tree species are
899 heterogeneously distributed between sapwood and heartwood. Environmental
900 Microbiology 20, 3744-3756.
901
902 Murray, A., Woodward, S., 2003. In vitro interactions between bacteria isolated from
903 Sitka spruce stumps and *Heterobasidion annosum*. Forest Pathology 33, 53-67.
904
905 Murray, A., Woodward, S., 2007. Temporal changes in functional diversity of
906 culturable populations in Sitka spruce stumps. Forest Pathology 37, 217-235.

Nicolitch, O., Colin, Y., Turpault, M.P., Uroz, S., 2016. Soil type determines the distribution of nutrient mobilizing bacterial communities in the rhizosphere of beech trees. Soil Biology and Biochemistry 103, 429-445.

Nicolitch, O., Colin, Y., Turpault, M.P., Fauchery, L., Uroz, S., 2017. Tree roots select specific bacterial communities in the subsurface critical zone. Soil Biology and Biochemistry 115, 109-123.

Noll L., Leonhardt, S., Arnstadt, T., Hoppe, B., Poll, C., Matzner, E., Hofrichter, M., Kellner, H., 2016. Fungal biomass and extracellular enzyme activities in coarse woody debris of 13 tree species in the early phase of decomposition. Forest Ecology Management 378, 181-192.

Oksanen, J., Kindt, R., Legendre, P., O'Hara, B., Stevens, M.H.H., Oksanen, M.J., Suggests M.A.S.S., 2007. The vegan package. Community ecology package 10, 631-637.

Olsen, S.R., 1954. Estimation of available phosphorus. In soils by extraction with sodium bicarbonate. US Department of Agriculture 939, 1-19.

Pan, Y., Birdsey, R.A., Fang, J., Houghton, R., Kauppi, P.E. Kurz, W.A. *et al.*, 2011. A large and persistent carbon sink in the world's forests. Science 333, 988–93.

Paradis, E., Claude, J., Strimmer, K., 2004 APE: analyses of phylogenetics and evolution in R language. Bioinformatics 20, 289-290.

Prewitt, L., Kang, Y., Kakumanu, M.L., Williams, M., 2014. Fungal and bacterial community succession differs for three wood types during decay in a forest soil. Microbial Ecology 68, 212-221.

Probst, M., Gómez-Brandón, M., Bardelli, T., Egli, M., Insam, H., Ascher-Jenull, J., 2018. Bacterial communities of decaying Norway spruce follow distinct slope exposure and time-dependent trajectories. Environmental Microbiology 20, 3657-3670.

Quast, C., Pruesse, E., Yilmaz, P., Gerken, J., Schweer, T., Yarza, P., Peplies, J., Glöckner, FO., 2012. The SILVA ribosomal RNA gene database project: improved data processing and web-based tools. Nucleic Acids Research 41, D590-D596.

R Core Team., 2015. R: a Language and Environment for Statistical Computing.

Rajala, T., Peltoniemi, M., Pennanen, T., Mäkipää, R., 2012. Fungal community dynamics in relation to substrate quality of decaying Norway spruce (*Picea abies* L. Karst.) logs in boreal forests. FEMS Microbiology Ecology 81, 494-505.

Rajala, T., Tuomivirta, T., Pennanen, T., Mäkipää, R., 2015. Habitat models of wood-inhabiting fungi along a decay gradient of Norway spruce logs. Fungal Ecology 18, 48-55.

Ricker, M.C., Lockaby, B.G., Blosser, G.D., Conner, W.H., 2016. Rapid wood decay and nutrient mineralization in an old-growth bottomland hardwood forest. Biogeochemistry 127, 323-338.

Rinta-Kanto, J.M., Sinkko, H., Rajala, T., Al-Soud, W.A., Sørensen, S.J., Tamminen, M.V., Timonen, S., 2016. Natural decay process affects the abundance and community structure of Bacteria and Archaea in *Picea abies* logs. FEMS Microbiology Ecology 92, fiw087.

Rognes, T., Flouri, T., Nichols, B., Quince, C., Mahé, F., 2016. VSEARCH: a versatile open source tool for metagenomics. PeerJ. 4, e2584.

Schneider, T., Keiblinger, K. M., Schmid, E., Sterflinger-Gleixner, K., Ellersdorfer, G., Roschitzki, B., Richter, A., Eberl, L., Zechmeister-Boltenstern, S., Riedel, K. (2012). Who is who in litter decomposition? Metaproteomics reveals major microbial players and their biogeochemical functions. The ISME journal 6, 1749-1762.

Seibold, S., Bässler, C., Brandl, R., Gossner, M.M., Thorn, S., Ulyshen, M.D., Müller, J., 2015. Experimental studies of dead-wood biodiversity—a review identifying global gaps in knowledge. Biological Conservation 191, 139-149.

Seidl, R, Schelhaas, M-J, Rammer, W, Verkerk, P.J., 2014. Increasing forest disturbances in Europe and their impact on carbon storage. Nature Climate Change 4, 806-810.

Stokland J.N., Siitonen, J., Jonsson, B.G., 2012. Biodiversity in Dead Wood. Cambridge: Cambridge University Press.

Štursová, M., Žifčáková, L., Leigh, M.B., Burgess, R. Baldrian, P., 2012. Cellulose utilization in forest litter and soil: identification of bacterial and fungal decomposers. FEMS Microbiology Ecology 80, 735-746.

Sun, H., Terhonen, E., Kasanen, R., Asiegbu, F.O., 2014. Diversity and community structure of primary wood-inhabiting bacteria in boreal forest. Geomicrobiology Journal 31, 315-324.

Tláskal, V., Zrůstová, P., Vrška, T., Baldrian, P., 2017. Bacteria associated with decomposing dead wood in a natural temperate forest. FEMS Microbiology Ecology 93, fix157.

Ulyshen, M.D., 2016. Wood decomposition as influenced by invertebrates. Biological Reviews 91, 70-85.

Valášková, V., De Boer, W., Gunnewiek, P.J.K., Pospisek, M., Baldrian, P., 2009. Phylogenetic composition and properties of bacteria coexisting with the fungus *Hypholoma fasciculare* in decaying wood. The ISME Journal 3, 1218.

Větrovský, T., Steffen, K.T., Baldrian, P., 2014. Potential of cometabolic transformation of polysaccharides and lignin in lignocellulose by soil Actinobacteria. PLoS one 9, e89108.

van der Wal, A., Ottosson, E., De Boer, W., 2015. Neglected role of fungal community composition in explaining variation in wood decay rates. Ecology 96, 124-133.

Vorob'ev, A.V., de Boer, W., Folman, L.B., Bodelier, P.L., Doronina, N.V., Suzina, N.E., Trotsenko Y.A., Dedysh, S. N., 2009. *Methylovirgula ligni* gen. nov., sp. nov., an obligately acidophilic, facultatively methylotrophic bacterium with a highly divergent mxaF gene. International Journal of Systematic and Evolutionary Microbiology 59, 2538-2545.

Weedon, J.T., Cornwell, W.K., Cornelissen, J.H.C., Zanne, A.E., Wirth, C., Coomes. D.A., 2009. Global meta-analysis of wood decomposition rates: a role for trait variation among tree species? Ecological Letters 12, 45-56.

Wickham, H., 2009. ggplot2: elegant graphics for data analysis. New York: Springer.

Zhang, H.B., Yang, M.X., Tu, R., 2008. Unexpectedly high bacterial diversity in decaying wood of a conifer as revealed by a molecular method. International Biodeterioration *and* Biodegradation 62**,** 471-474.

A.

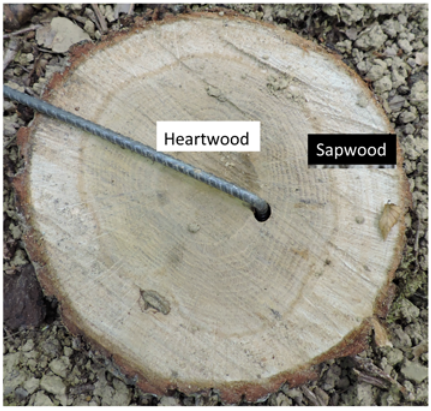
Heartwood
Sapwood

B.

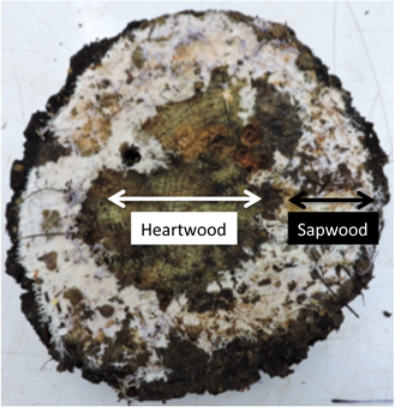
Heartwood
Sapwood

C.

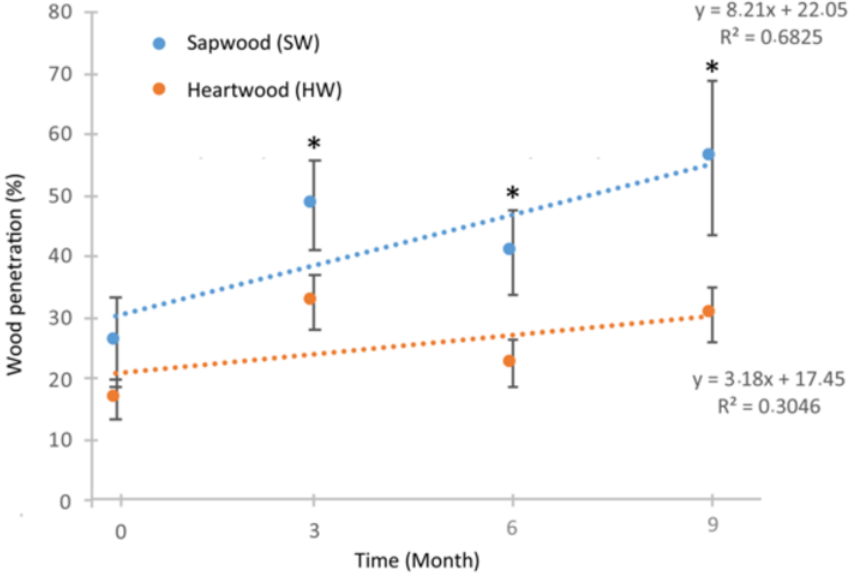
Sapwood (SW)
Heartwood (HW)
y = 8.21x + 22.05
R² = 0.6825
y = 3.18x + 17.45
R² = 0.3046
Wood penetration (%)
Time (Month)
0
10
20
30
40
50
60
70
80
0
3
6
9
*
*
*

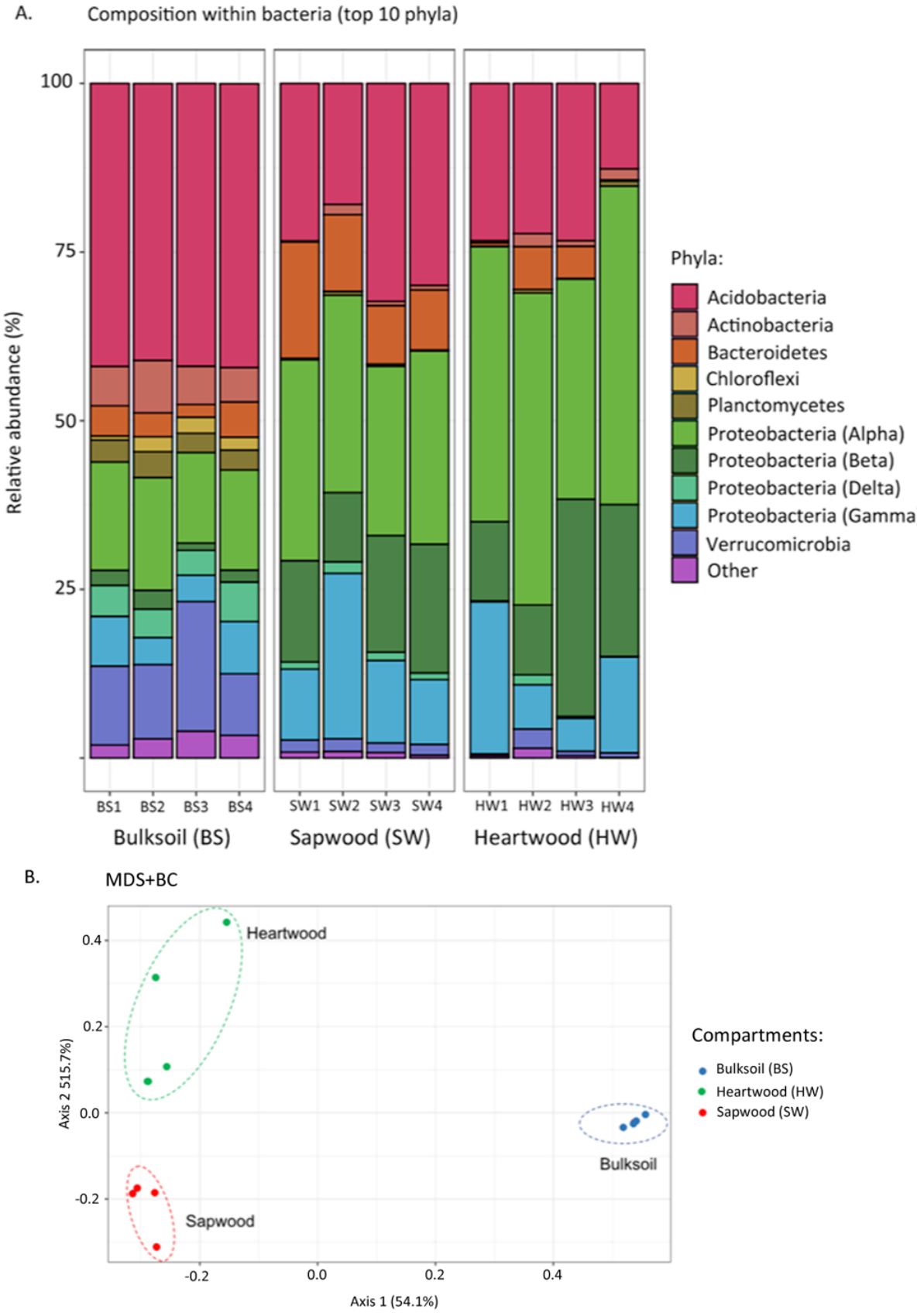
A.
Composition within bacteria (top 10 phyla)
Relative abundance (%)
100
75
50
25
BS1
BS2
BS3
BS4
SW1
SW2
SW3
SW4
HW1
HW2
HW3
HW4
Bulksoil (BS)
Sapwood (SW)
Heartwood (HW)
Phyla:
Acidobacteria
Actinobacteria
Bacteroidetes
Chloroflexi
Planctomycetes
Proteobacteria (Alpha)
Proteobacteria (Beta)
Proteobacteria (Delta)
Proteobacteria (Gamma)
Verrucomicrobia
Other
B.
MDS+BC
Heartwood
Bulksoil
Sapwood
0.4
0.2
0.0
-0.2
Axis 2 515.7%)
-0.2
0.0
0.2
0.4
Axis 1 (54.1%)
Compartments:
Bulksoil (BS)
Heartwood (HW)
Sapwood (SW)

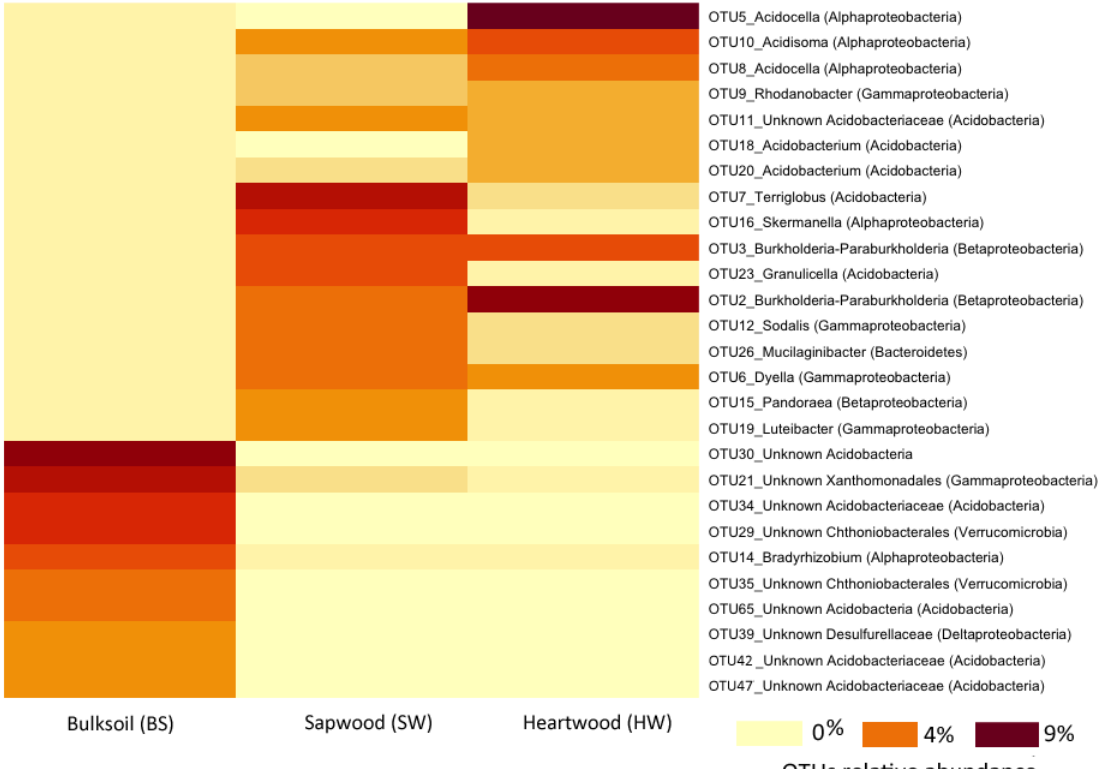
OTU5_Acidocella (Alphaproteobacteria)
OTU10_Acidisoma (Alphaproteobacteria)
OTU8_Acidocella (Alphaproteobacteria)
OTU9_Rhodanobacter (Gammaproteobacteria)
OTU11_Unknown Acidobacteriaceae (Acidobacteria)
OTU18_Acidobacterium (Acidobacteria)
OTU20_Acidobacterium (Acidobacteria)
OTU7_Terriglobus (Acidobacteria)
OTU16_Skermanella (Alphaproteobacteria)
OTU3_Burkholderia-Paraburkholderia (Betaproteobacteria)
OTU23_Granulicella (Acidobacteria)
OTU2_Burkholderia-Paraburkholderia (Betaproteobacteria)
OTU12_Sodalis (Gammaproteobacteria)
OTU26_Mucilaginibacter (Bacteroidetes)
OTU6_Dyella (Gammaproteobacteria)
OTU15_Pandoraea (Betaproteobacteria)
OTU19_Luteibacter (Gammaproteobacteria)
OTU30_Unknown Acidobacteria
OTU21_Unknown Xanthomonadales (Gammaproteobacteria)
OTU34_Unknown Acidobacteriaceae (Acidobacteria)
OTU29_Unknown Chthoniobacterales (Verrucomicrobia)
OTU14_Bradyrhizobium (Alphaproteobacteria)
OTU35_Unknown Chthoniobacterales (Verrucomicrobia)
OTU65_Unknown Acidobacteria (Acidobacteria)
OTU39_Unknown Desulfurellaceae (Deltaproteobacteria)
OTU42_Unknown Acidobacteriaceae (Acidobacteria)
OTU47_Unknown Acidobacteriaceae (Acidobacteria)
Bulksoil (BS)
Sapwood (SW)
Heartwood (HW)
0%
4%
9%
OTUs relative abundance

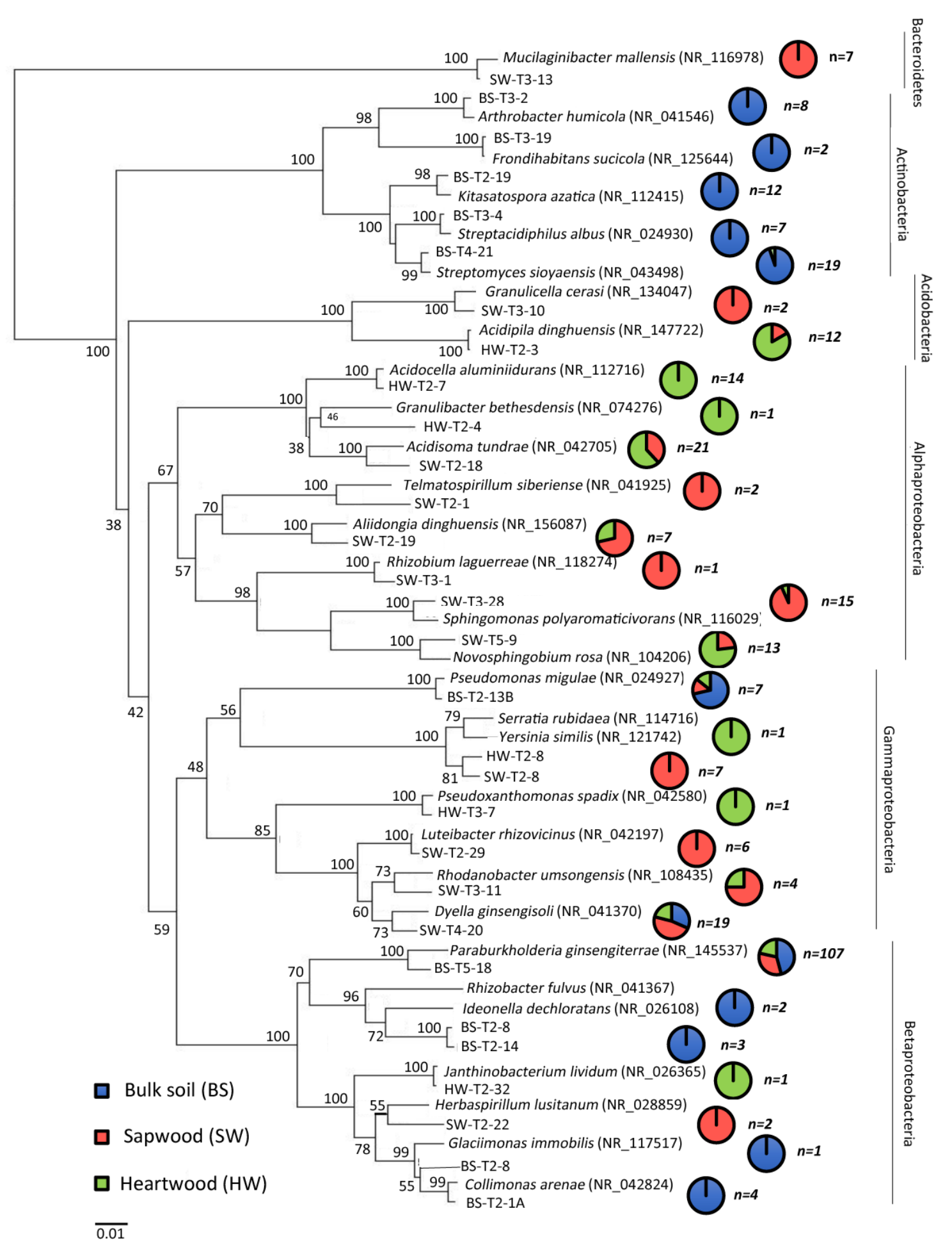
Mucilaginibacter mallensis (NR_116978)
SW-T3-13
BS-T3-2
Arthrobacter humicola (NR_041546)
BS-T3-19
Frondihabitans sucicola (NR_125644)
BS-T2-19
Kitasatospora azatica (NR_112415)
BS-T3-4
Streptacidiphilus albus (NR_024930)
BS-T4-21
Streptomyces sioyaensis (NR_043498)
Granulicella cerasi (NR_134047)
SW-T3-10
Acidipila dinghuensis (NR_147722)
HW-T2-3
Acidocella aluminiidurans (NR_112716)
HW-T2-7
Granulibacter bethesdensis (NR_074276)
HW-T2-4
Acidisoma tundrae (NR_042705)
SW-T2-18
Telmatospirillum siberiense (NR_041925)
SW-T2-1
Aliidongia dinghuensis (NR_156087)
SW-T2-19
Rhizobium laguerreae (NR_118274)
SW-T3-1
SW-T3-28
Sphingomonas polyaromaticivorans (NR_116029)
SW-T5-9
Novosphingobium rosa (NR_104206)
Pseudomonas migulae (NR_024927)
BS-T2-13B
Serratia rubidaea (NR_114716)
Yersinia similis (NR_121742)
HW-T2-8
SW-T2-8
Pseudoxanthomonas spadix (NR_042580)
HW-T3-7
Luteibacter rhizovicinus (NR_042197)
SW-T2-29
Rhodanobacter umsongensis (NR_108435)
SW-T3-11
Dyella ginsengisoli (NR_041370)
SW-T4-20
Paraburkholderia ginsengiterrae (NR_145537)
BS-T5-18
Rhizobacter fulvus (NR_041367)
Ideonella dechloratans (NR_026108)
BS-T2-8
BS-T2-14
Janthinobacterium lividum (NR_026365)
HW-T2-32
Herbaspirillum lusitanum (NR_028859)
SW-T2-22
Glaciimonas immobilis (NR_117517)
BS-T2-8
Collimonas arenae (NR_042824)
BS-T2-1A
n=7
n=8
n=2
n=12
n=7
n=19
n=2
n=12
n=14
n=1
n=21
n=2
n=7
n=1
n=15
n=13
n=7
n=1
n=7
n=1
n=6
n=4
n=19
n=107
n=2
n=3
n=1
n=2
n=1
n=4
Bacteroidetes
Actinobacteria
Acidobacteria
Alphaproteobacteria
Gammaproteobacteria
Betaproteobacteria
Bulk soil (BS)
Sapwood (SW)
Heartwood (HW)
0.01

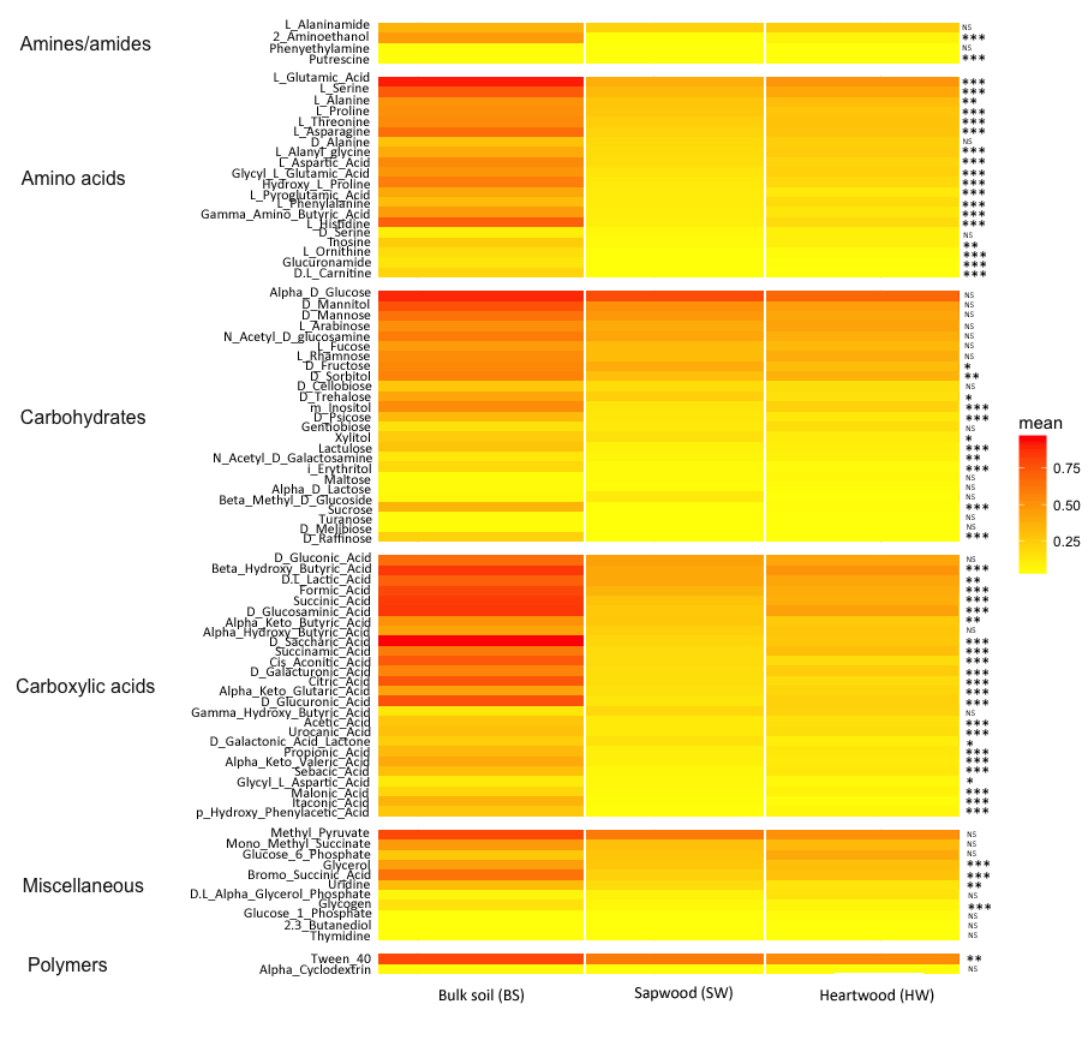
Amines/amides
L_Alaninamide
2_Aminoethanol
Phenyethylamine
Putrescine
NS
***
NS
***
Amino acids
L_Glutamic_Acid
L_Serine
L_Alanine
L_Proline
L_Threonine
L_Asparagine
D_Alanine
L_Alanyl_glycine
L_Aspartic_Acid
Glycyl_L_Glutamic_Acid
Hydroxy_L_Proline
L_Pyroglutamic_Acid
L_Phenylalanine
Gamma_Amino_Butyric_Acid
L_Histidine
D_Serine
Tirosine
L_Ornithine
Glucuronamide
D,L_Carnitine
***
***
**
***
***
***
NS
***
***
***
***
***
***
***
NS
**
***
***
***
Carbohydrates
Alpha_D_Glucose
D_Mannitol
D_Mannose
L_Arabinose
N_Acetyl_D_glucosamine
L_Fucose
L_Rhamnose
D_Fructose
D_Sorbitol
D_Cellobiose
D_Trehalose
m_Inositol
D_Psicose
Gentiobiose
Xylitol
Lactulose
N_Acetyl_D_Galactosamine
i_Erythritol
Maltose
Alpha_D_Lactose
Beta_Methyl_D_Glucoside
Sucrose
Turanose
D_Melibiose
D_Raffinose
NS
NS
NS
NS
NS
NS
NS
*
**
NS
*
***
***
NS
*
***
**
***
NS
NS
NS
***
NS
NS
***
mean
0.75
0.50
0.25
Carboxylic acids
D_Gluconic_Acid
Beta_Hydroxy_Butyric_Acid
D,L_Lactic_Acid
Formic_Acid
Succinic_Acid
D_Glucosaminic_Acid
Alpha_Keto_Butyric_Acid
Alpha_Hydroxy_Butyric_Acid
D_Saccharic_Acid
Succinamic_Acid
Cis_Aconitic_Acid
D_Galacturonic_Acid
Citric_Acid
Alpha_Keto_Glutaric_Acid
D_Glucuronic_Acid
Gamma_Hydroxy_Butyric_Acid
Acetic_Acid
Urocanic_Acid
D_Galactonic_Acid_Lactone
Propionic_Acid
Alpha_Keto_Valeric_Acid
Sebacic_Acid
Glycyl_L_Aspartic_Acid
Malonic_Acid
Itaconic_Acid
p_Hydroxy_Phenylacetic_Acid
NS
***
**
***
***
***
**
NS
***
***
***
***
***
***
***
NS
***
***
***
***
*
***
***
***
Miscellaneous
Methyl_Pyruvate
Mono_Methyl_Succinate
Glucose_6_Phosphate
Glycerol
Bromo_Succinic_Acid
Uridine
D,L_Alpha_Glycerol_Phosphate
Glycogen
Glucose_1_Phosphate
2,3_Butanediol
Thymidine
NS
NS
NS
***
***
**
NS
***
NS
NS
NS
Polymers
Tween_40
Alpha_Cyclodextrin
**
NS
Bulk soil (BS)
Sapwood (SW)
Heartwood (HW)

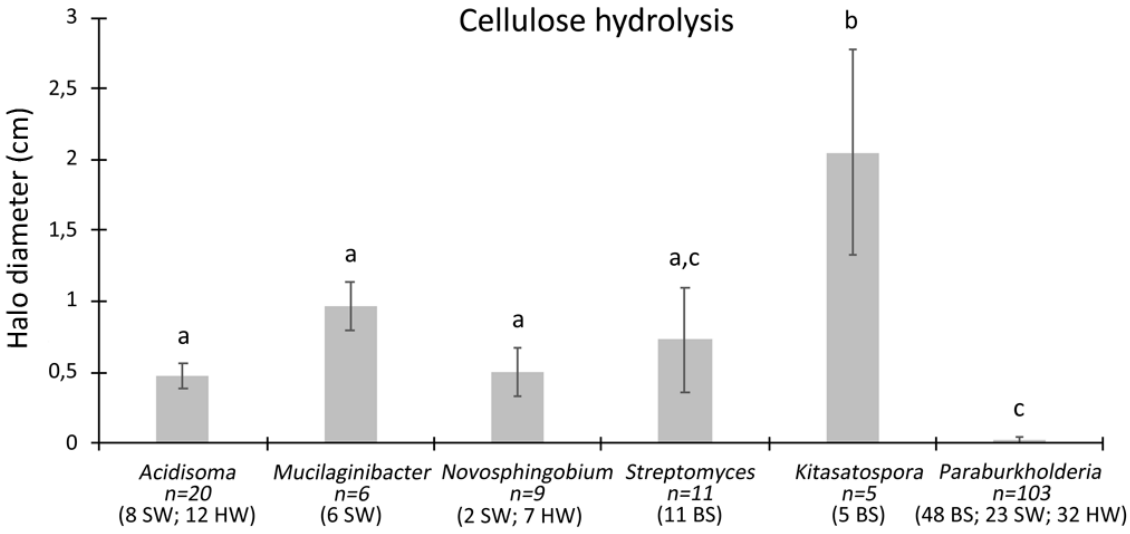
Cellulose hydrolysis
Halo diameter (cm)
3
2,5
2
1,5
1
0,5
0
a
a
a
a,c
b
c
Acidisoma
n=20
(8 SW; 12 HW)
Mucilaginibacter
n=6
(6 SW)
Novosphingobium
n=9
(2 SW; 7 HW)
Streptomyces
n=11
(11 BS)
Kitasatospora
n=5
(5 BS)
Paraburkholderia
n=103
(48 BS; 23 SW; 32 HW)

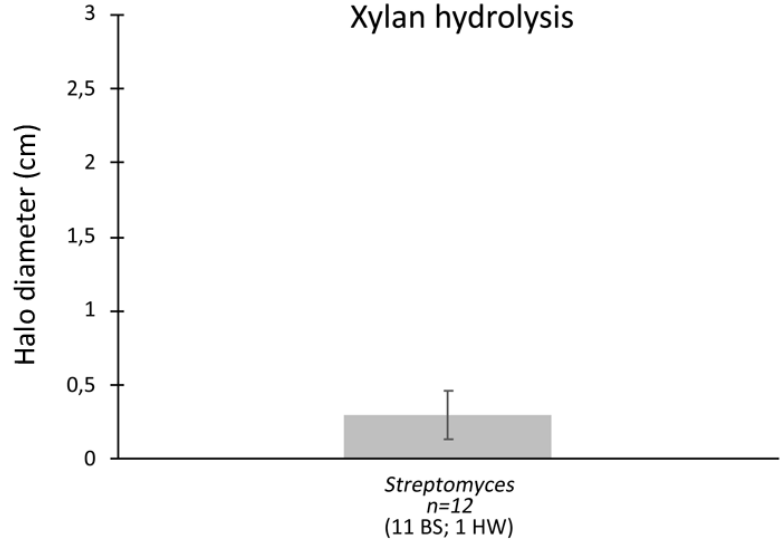
Xylan hydrolysis
Halo diameter (cm)
3
2,5
2
1,5
1
0,5
0
Streptomyces
n=12
(11 BS; 1 HW)

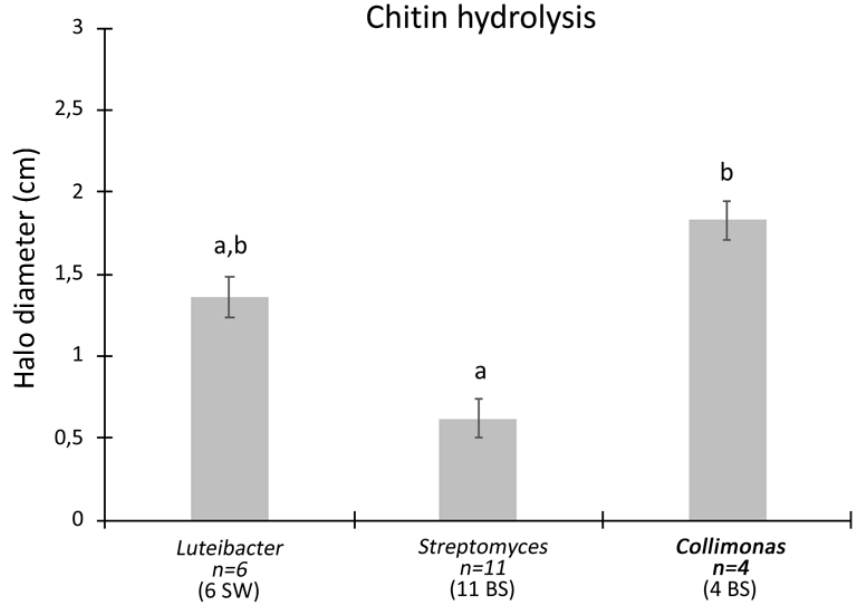
Chitin hydrolysis
Halo diameter (cm)
3
2,5
2
1,5
1
0,5
0
a,b
a
b
Luteibacter
n=6
(6 SW)
Streptomyces
n=11
(11 BS)
Collimonas
n=4
(4 BS)

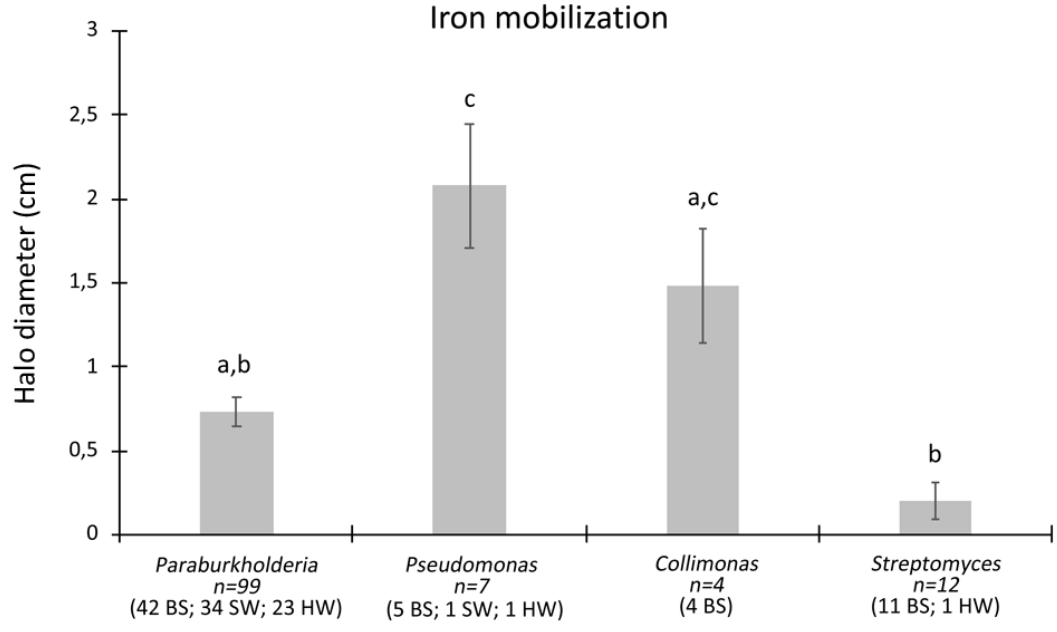
Iron mobilization
Halo diameter (cm)
3
2,5
2
1,5
1
0,5
0
a,b
c
a,c
b
Paraburkholderia
n=99
(42 BS; 34 SW; 23 HW)
Pseudomonas
n=7
(5 BS; 1 SW; 1 HW)
Collimonas
n=4
(4 BS)
Streptomyces
n=12
(11 BS; 1 HW)